Exact Solution, Endoreversible Thermodynamics, and Kinetics of the Generalized Shockley-Queisser Model

Andrei Sergeev and Kimberly Sablon

Phys. Rev. Applied **10**, 064001 — Published 3 December 2018

DOI: 10.1103/PhysRevApplied.10.064001

Exact Solution, Endoreversible Thermodynamics, and Kinetics of the Generalized Shockley-Queisser Model

Andrei Sergeev*
U.S. Army Research Laboratory, Adelphi, Maryland 20783, USA

Kimberly Sablon
Office of the Deputy Assistant Secretary of the Army for Research and Technology, USA
(Dated: October 23, 2018)

We consider the generalized Shockley-Queisser (gSQ) model, which is based on a single assumption that photocarriers and emitted photons are in chemical equilibrium and described by the Boltzmann distribution functions with the same chemical potential. The model takes into account the frequency dependent absorption (emission), photon trapping and recycling, photocarriers multiplication, and nonradiative recombination processes. For the non-interacting photocarriers, we obtain *exact analytical* solution of gSQ model and present the conversion efficiency, and other photovoltaic (PV) characteristics in convenient form via the Lambert W function. Photocarrier multiplication and recombination via three-body Auger processes are also directly included in this formalism. We derive universal formulas for useful energy, thermal losses, and emission losses per absorbed photon. We show that the relation between the maximal conversion efficiency and the photo-induced chemical potential, obtained by Henry [1] for the ideal SQ limit, is also valid in gSQ model. In the general case of interacting electrons, in particular for the Shockley-Read-Hall processes, the solution is presented in the iterative form. We analyze photocarrier kinetics and derive a general relation between the optimal photocarrier collection time and photocarrier lifetime with respect to all radiative and nonradiative processes. Finally, we analyze finite mobility limitations and show that PV devices with photon trapping and recycling provide fast photocarrier collection required by gSQ model.

Introduction

In 1960 Shockley and Queisser developed fundamental model of photovoltaic (PV) conversion in a semiconductor single-junction solar cell and numerically calculated the maximal conversion efficiency in terms of detailed balance between the absorbed and emitted photon fluxes [2]. Initially, the paper was rejected as trivial and unrelated to real semiconductors [3, 4]. During the APS March Meeting in 1960, the scientists participating in the discussion agreed that the SQ theory may be applicable to at least GaAs with weak non-radiative recombination processes. Now the Shockley-Queisser (SQ) limiting efficiencies are considered as the most fundamental benchmarks in solar light conversion. Besides benchmarking characteristics of PV devices, two fundamental problems related to radiative SQ limit are hot topics of modern theoretical research. The first problem is the derivation of the SQ limit from general theoretical concepts. The SQ limit is investigated in frame of classical thermodynamics [5], endoreversible thermodynamics [6, 7], and nonequilibrium thermodynamics [8]. The second problem is the possibility to overcome SQ limit due to photonic management [9–11] and nano-enhanced thermophotovoltaic conversion [12]. Despite hundreds of works devoted to the SQ model, even for the ideal model without nonradiative processes the analytical solution has not been found yet. Recent work [13] with tabulated values of the SQ PV characteristics for traditional single junction solar cell is widely used for benchmarking solar cell parameters.

Nonraditiave processes substantially complicate description of PV conversion. Currently, interplay of radiative and nonradiative processes in the open-circuit regime is understood substantially better than that in the regime with optimal conversion of electromagnetic power. First, the open-circuit regime provides the maximal output electric energy with the conversion time goes to infinity and, therefore, it is well described by classical thermodynamics. For narrow-band radiation above the semiconductor bandgap, thermodynamics establishes the Carnot limit (Carnot loss) for the open-circuit voltage. Irreversible processes due to energy relaxation of photocarriers created by wide spectrum radiation may be also incorporated in the thermodynamic approach as thermalization losses [14]. Second, there is exact analytical solution for the open-circuit voltage (output energy) as a function of spectral and geometrical characteristics of the photon flux. The analytical solution has been generalized to include other losses due to nonradiative recombination processes in terms of luminescence quantum yield [14–16] and also to include light management in terms of photon trapping/recycling [17, 18]. Therefore, analysis of the open circuit regime is very often employed for optimization of electron and photon processes related to PV conversion [9–11, 17, 18].

The conversion regime with optimal output power is described by the endoreversible thermodynamics, which includes irreversible processes and entropy generation due to thermal energy transfer from the radiation source to the solar cell. Despite extensive theoretical research, the analytical expression for the maximal output elec-

*Corresponding author: podolsk37@gmail.com

tric power (the power conversion efficiency) as a function of photon flux characteristics has not been obtained yet. The regime of optimal power conversion is currently investigated via numerical modeling, which limit our understanding of complex electron, photon, and phonon processes and their interplay in this regime.

In this work we consider the generalized Shockley-Queisser (gSQ) model which takes into account absorption/emission characteristics and nonradiative recombination processes, which limit the photocarrier collection. We derive analytical solution of gSQ model and present the PV efficiency and other thermodynamic and kinetic characteristics in simple and convenient form. The paper is organized in the following way. In the next Section we formulate the generalized Shockley - Queisser model. In Section III the analytical expression for useful power (conversion efficiency) for non-interacting electrons will be derived. In this section we also discuss corresponding relations of endoreversible thermodynamics and present the useful energy of a photon via the photo-induced chemical potential. In Section IV the obtained solution is generalized to include Auger recombination processes and photon recycling. In Section V we present a general perturbative solution for the interacting electrons. In particular, the Shockley-Read-Hall recombination is analyzed. In Section V we consider photocarrier kinetics and obtain a universal relation between the optimal photocarrier collection time and the photocarrier lifetime due to all radiative and nonradiative processes as a function of photon flux characteristics. We found that in typical solar cells (Si, GaAs etc) the optimal collection time of photocarriers should be shorter than the photocarrier lifetime by 20 - 50 times depending on solar light concentration, semiconductor bandgap, and nonradiative recombination rate. In Section VI we analyze the limitations of the generalized Shockley-Queisser model related to the finite photocarrier mobility, which can limit the optimal photocarrier collection rate, calculated in the previous section. We conclude that in the semiconductor PV devices with photon trapping and recycling the optimal device thickness is below the critical value that limits the photocarrier collection by diffusion processes. Thus, the presented generalized Shockley-Queisser model and its analytical solution for useful power (efficiency), thermodynamic and kinetic characteristics provide very effective tool for design and optimization of modern thin PV devices with back-surface mirror (recycling) and front photon scattering (trapping) with simple mathematical software. Moreover, as the large-argument asymptotic of Lambert W function is accurately presented by three logarithmic terms (see Section II), the corresponding characteristics may be calculated by using relatively simple scientific calculators. In Section VII, we will apply the developed formalism to analysis of GaAs solar operating close to SQ limit. The developed general mathematical formalism for PV conversion may be very useful for analysis of perspectives of new PV materials and novel PV concepts.

II. Generalized Shockley - Queisser Model

The SQ model is based on the three-stage photocarrier kinetics in a semiconductor. At the first stage the light-induced carriers strongly interact with phonons. Due to emission of high-energy phonons, the photocarriers lose energy and relax to the band-edges. Then, the photocarriers accumulated near band-edges absorb and emit thermal phonons. The phonon emission and absorption processes establish the electron and hole distributions, which are described by the equilibrium temperature and nonequilibrium chemical potentials, i.e $f_{e(h)} = [\exp(\epsilon - \mu_{e(h)})/kT + 1]^{-1}$ with the chemical potentials $\mu_{e(h)}$ independent on ϵ. To simplify presentation, we will consider a doped semiconductor, where light absorption mainly increases the chemical potential of minority carriers. At the second stage the photocarriers recombine and emit photons that are described by the temperature T and the light-induced chemical potential μ of minority carriers, i.e the distribution of emitted photons is given by $f_{ph} = [\exp(h\nu - \mu)/kT - 1]^{-1}$. The emitted photons may be reabsorbed and create the electron-hole pairs again. The reabsorption process increases the lifetime of minority photocarriers. At the third stage, a stationary value of the light-induced chemical potential is established due to carrier collection at the device contacts and due to photon escape from the device. The stationary photon and photocarrier distribution functions, may be approximated by the quasi-classical distribution, $f_{ph} = \exp[(\mu - h\nu)/kT]$ and $f_e = \exp[(\mu - \epsilon)/kT]$, because even in the case of the maximal solar light concentration the light induced chemical potential is substantially below the bandgap and the parameter $(\epsilon - \mu)/kT$ is much larger than 1.

The quasi-classical function may be factorized as $\exp(\mu/kT) \times \exp(-h\omega/kT)$ and, therefore, the photon flux emitted by the cell into the medium with the refractive index n may be presented as

$$\begin{aligned} \dot{N}_{em}(\mu, T) &= \exp\frac{\mu}{kT} \int \frac{c}{4n}\sigma(\omega) D_\omega \exp\left(-\frac{\hbar\omega}{kT}\right) d\omega \\ &= \exp\frac{\mu}{kT} \cdot \dot{N}_{em}(T), \end{aligned} \tag{1}$$

where $\dot{N}_{em}(T)$ is the emitted flux in equilibrium ($\mu = 0$), c the speed of light in vacuum, $\sigma(\omega)$ is the emissivity of the solar cell interface and, in accordance with the Kirchhoff law, also its absorptivity. The photon density of states, D_ω, is given by

$$D_\omega = \frac{n^3\omega^2}{\pi^2 c^3}. \tag{2}$$

The electric current density is determined by the difference between the generation and recombination rates,

$$J/q = \dot{G} - \dot{R}, \tag{3}$$

where q is the electron charge. The generation rate is given by $\dot{G} = \gamma \dot{N}_{ab}$, where N_{ab} is the absorbed photon

flux and γ is photocarrier multiplication coefficient due to inverse Auger processes [19]. The radiative recombination rate is proportional to the density of minority carriers and determines the photon emission flux. In accordance with Eq. 1, the radiative recombination rate may be factorized as

$$\dot{R}_r = \dot{N}_{em}(\mu, T) = \exp(\mu/kT) \cdot \dot{N}_{em}(T). \tag{4}$$

Following to Ross [14], we present the total recombination rate due to all radiative and nonradiative processes through the luminescence quantum yield k_l as

$$\dot{R} = \frac{\dot{R}_r}{k_l} = \frac{\dot{N}_{em}(T)}{k_l} \cdot \exp\frac{\mu}{kT}. \tag{5}$$

The approximation of nonradiative losses by the luminescence quantum yield assumes fast relaxation of light induced photocarriers and the time reversal electron transport in regimes of photocarrier collection (solar cell) and carrier injection for light generation (LED). Time reversibility of electron transport in p-n junction devices has been discussed in recent papers [15, 16]. As it was pointed out by Ross [14], for non-interacting photocarriers the luminescence quantum yield k_l is independent on photocarrier concentration and, therefore, chemical potential, μ. Thus, according to Eqs. 3-5, for non-interacting electrons the photo-induced electric current is given by

$$J/q = \gamma \dot{N}_{ab} - \frac{\dot{N}_{em}(T)}{k_l} \cdot \exp\frac{\mu}{kT}. \tag{6}$$

Taking into account that the useful energy per electron is μ, the photovoltaic conversion efficiency is given by

$$\begin{aligned} \eta &= \frac{\mu(J/q)}{\dot{E}_{in}} = \left(\gamma \dot{N}_{ab} - \frac{\dot{N}_{em}(T)}{k_l} \cdot \exp\left(\frac{\mu}{kT}\right)\right) \cdot \frac{\mu}{\dot{E}_{in}} \\ &= \left(\gamma - \frac{\dot{N}_{em}(T)}{k_l \cdot \dot{N}_{ab}} \cdot \exp\left(\frac{\mu}{kT}\right)\right) \cdot \frac{\mu}{\epsilon^*}, \end{aligned} \tag{7}$$

where $\dot{E}_{in}$ is the power of incoming photon flux and $\epsilon^* = \dot{E}_{in}/\dot{N}_{ab}$ is the average energy in the flux per a photon absorbed in solar cell. This characteristic photon energy may be also presented as $\epsilon^* = \tilde{\epsilon}/\tilde{\alpha}$, where $\tilde{\epsilon}$ is average photon energy in the flux and $\tilde{\alpha} = \dot{N}_{ab}/\dot{N}_{flux}$ is absorptance of the cell. As an example, Fig. 1 shows the parameter ϵ^* as a function of the bandgap for the 6000 K thermal radiation and 100 % absorption above the bandgap.

III. Analytical Solution and Endoreversible Thermodynamics for Non-interacting Electrons

Introducing the dimensionless parameter,

$$A = \frac{k_l \dot{N}_{ab}}{\dot{N}_{em}(T)}, \tag{8}$$

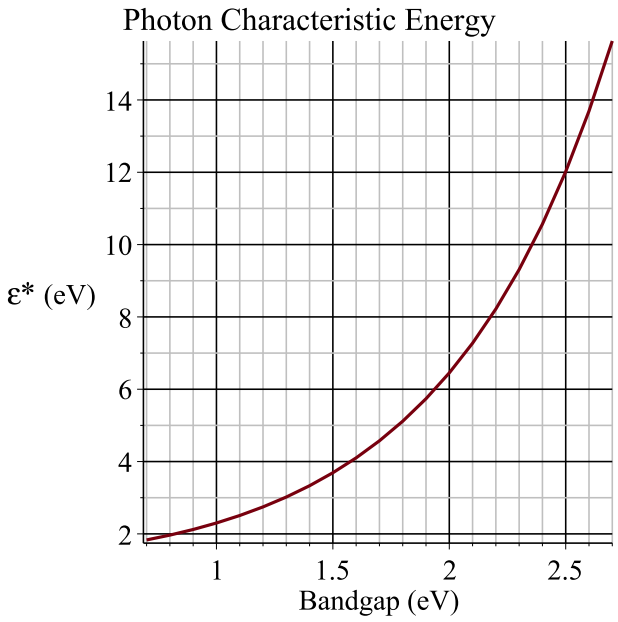

FIG. 1: Average energy per a photon, ϵ^*, for the 6000 K radiation flux as a function of semiconductor bandgap (100% absorption above the bandgap).

and by optimizing the efficiency as a function of the chemical potential (Eq. 7), we obtain the following equation for the chemical potential (output voltage) at maximal PV efficiency,

$$\left(\frac{\mu_m}{kT} + 1\right) \cdot \exp\frac{\mu_m}{kT} = \gamma \cdot A \tag{9}$$

This transcendental equation has analytical solution in terms of the Lambert W function,

$$\frac{\mu_m}{kT} = \frac{qV_m}{kT} = \mathrm{LW}(\gamma \cdot A \cdot e) - 1, \tag{10}$$

where V_m is the voltage at maximal output power, LW is used for the Lambert W function and $e = 2.71828$ is Euler's number. Substituting μ_m to the equation for the conversion efficiency (Eq. 1), we find the maximal conversion efficiency,

$$\eta_m = \gamma \left[\mathrm{LW}(\gamma \cdot A \cdot e) - 2 + \frac{1}{\mathrm{LW}(\gamma \cdot A \cdot e)}\right] \cdot \frac{kT}{\epsilon^*}. \tag{11}$$

Thus, the output electric power is given by

$$P_e = \gamma \left[\mathrm{LW}(\gamma \cdot A \cdot e) - 2 + \frac{1}{\mathrm{LW}(\gamma \cdot A \cdot e)}\right] kT \cdot \dot{N}_{abs}. \tag{12}$$

Eqs. 10, 11 and 12 represent *exact analytical* solution of gSQ model for non-interacting electrons and express the conversion efficiency and output electric power through the absorption coefficient, $\sigma(\nu)$, the photocarrier multiplication coefficient, γ, and the luminescent yield, k_l.

Using Eqs. 10 and 12 we obtained the general relation between the maximal output power and the output voltage at maximal conversion efficiency,

$$P_e = \gamma \frac{(qV_m)^2}{qV_m + kT} \cdot \dot{N}_{ab}. \quad (13)$$

Eq. 13 generalizes the relation obtained by Henry [1] for ideal light absorption and absence of nonradiative processes ($\sigma(\nu) = k_l = \gamma = 1$). It shows that the useful energy per absorbed photon, $\gamma(qV_m)^2/(qV_m + kT)$, is independent on the electron-hole recombination mechanisms.

Now we obtain some useful general relations of the endoreversible thermodynamics of PV conversion. Substituting the solution given by Eq. 10 into Eq. 4, we find the photon emission flux at maximal efficiency,

$$\dot{N}_{em} = \frac{\gamma k_l \cdot kT}{qV_m + kT} \cdot \dot{N}_{ab} = \frac{\gamma k_l}{LW(\gamma \cdot A \cdot e)} \cdot \dot{N}_{ab}. \quad (14)$$

Therefore, the power of the emitted flux is given by

$$P_{em} = \frac{\gamma k_l \cdot kT}{qV_m + kT} \cdot \epsilon(T) \cdot \dot{N}_{ab}, \quad (15)$$

where $\epsilon(T)$ is the average photon energy in the emitted flux in thermodynamic equilibrium ($\mu = 0$) calculated with real frequency-dependent emissivity (absorptivity) of the material. Finally, the total thermal power generated in relaxation and nonradiative recombination processes may be presented as,

$$P_{th} = \left(\epsilon^* - \gamma \frac{(qV_m)^2 + k_l \cdot kT \cdot \epsilon(T)}{qV_m + kT} \right) \cdot \dot{N}_{ab}. \quad (16)$$

Naturally, in thermal equilibrium between the radiation source and PV device, the thermal power generated in the cell, P_{th}, is zero, because the photo-induced chemical potential is zero and, in accordance with Kirchhoff law, $\epsilon^* = \epsilon(T)$. Let us highlight, that the equations above directly show which part of the photon energy is converted into electric energy (Eq. 13) and into the heat (Eq. 16) and which part of the photon energy is emitted back (Eq. 15) in accordance with the detailed balance.

Finally, let us note that usually in PV conversion the ratio of the generation rate to the equilibrium recombination rate is huge. For large of the parameter A in Eqs. 10-12, one can use asymptotic formula for the Lambert W function [20, 21],

$$\begin{aligned} \mathrm{LW}(z) &= L_1 - L_2 + \frac{L_2}{L_1} + \frac{L_2(L_2-2)}{L_1^2} \\ &+ \frac{L_2(6 - 9L_2 + 2L_2^2)}{6L_1^3} + ... \quad (17) \\ L_1 &= \ln(z)\ ,\ L_2 = \ln\ln(z). \end{aligned}$$

First three terms in this asymptotic present LW function with the accuracy of $\sim (\ln\ln(z)/\ln(z))^2$, which is for typical values of A is $\sim 0.1\%$. This asymptotic formula may be used to calculate the efficiency and other characteristics in the optimal conversion regime using a scientific calculator.

Taking into account the asymptotic expression for the Lambert W function and neglecting the terms of the order of $1/\ln(A)$, we can simplify Eqs. 10 and 11. With $1/\ln(A)$ accuracy, we get

$$\begin{aligned} qV_m &= \mu_m = kT \cdot \mathrm{LW}(\gamma \cdot A), \quad (18) \\ \eta_m &= \gamma \left[\mathrm{LW}(\gamma \cdot A) - 1\right] \cdot \frac{kT}{\epsilon^*}. \quad (19) \end{aligned}$$

PV characteristics may be presented via the open circuit voltage,

$$qV_{oc} = \mu_{oc} = kT \cdot \ln(\gamma A). \quad (20)$$

The voltage at maximum efficiency is given by

$$\begin{aligned} V_M &= \frac{kT}{q} \cdot [\mathrm{LW}(\gamma A e) - 1] \\ &\approx V_{oc} - \frac{\ln(qV_{oc}/kT)}{q/kT} + \frac{\ln(qV_{oc}/kT) - 1}{q^2 V_{oc}/(kT)^2} \quad (21) \end{aligned}$$

Solution of the SQ model for the PV efficiency (Eq. 11) also provides a simple formula for the fill factor,

$$\begin{aligned} FF &\equiv \frac{\eta \dot{E}_{in}}{J_{sc} \cdot V_{oc}} = \frac{\mathrm{LW}(\gamma A e) - 2 + 1/\mathrm{LW}(\gamma A e)}{(1 - 1/\gamma A) \cdot \ln(\gamma A)} \\ &\approx 1 - \frac{\ln(qV_{oc}/kT) + 1}{qV_{oc}/kT} + \frac{\ln(qV_{oc}/kT)}{(qV_{oc}/kT)^2}. \quad (22) \end{aligned}$$

The asymptotic formulas in Eqs. 21 and 22 are presented in accordance with Eq. 17 as series of $L_2/L_1 = \ln\ln(\gamma A)/\ln(\gamma A) = kT/qV_{oc} \cdot \ln(qV_{oc}/kT)$, which are in good agreement with well-known asymptotic and empirical formulas derived by Green [22, 23] The Lambert W function is a built-in function in all mathematical packages (Maple, MATLAB, Maxima, Mathematica etc) [24] and, therefore, the obtained exact analytical solution drastically simplifies calculation of all PV characteristics. Fig. 2 shows the results of such calculations for concentrated and unconcentrated 6000 K radiation and different values of luminescence quantum yield.

IV. Auger Processes and Photon Recycling

In this Section we consider Auger recombination and its enhancement due to photon recycling. The phonon emission from the PV junction is realized from the front air-film interface and from the back film-substrate interface. Therefore, the total flux (Eq. 1) emitted by the PV junction may be presented as

$$\dot{N}_{em} = \dot{N}_{a-f} + \dot{N}_{f-s} \quad (23)$$

The number of thermally excited photon modes in the semiconductor structure of thickness d is

$$N(T,d) = d \cdot \int d\omega\ D_\omega f_{ph}(\omega), \quad (24)$$

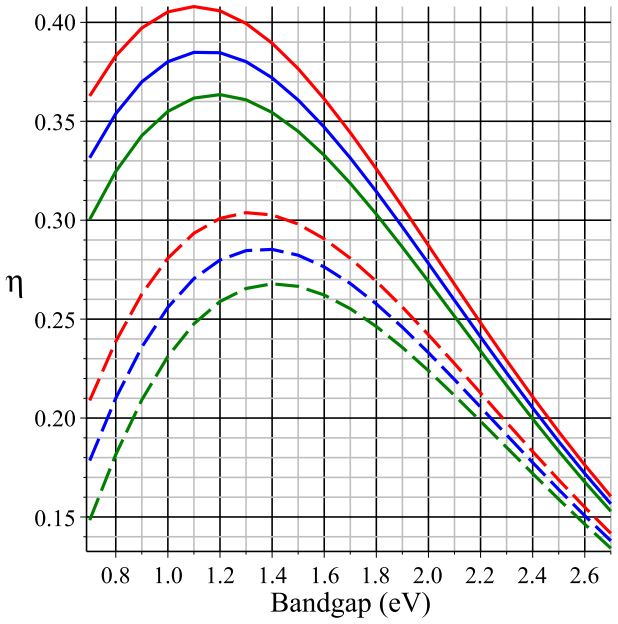

FIG. 2: PV conversion efficiencies given by Eq. 11 for the solar cells with the luminescence quantum yield of 100% (red), 10% (blue) and 1% (green) under concentrated solar light (solid lines) and unconcentrated light (dashed lines).

whereD_ω is the photon density of states (Eq. 2) and $f_{ph}(\omega)$ is the Plank distribution function. Slow photon escape (emission) through the film-air interface results from internal reflection of photon modes outside the escape cone with the angle θ_{es}, where $\sin\theta_{es} = 1/n$. Therefore, the rate of photon emission from the film to air is given by

$$\dot{N}_{f-a}(T) = (\tilde{c}/4)(\sin\theta_{es})^2\ \kappa\cdot\int d\omega\ D_{ph}(\omega)\ f_{ph}(\omega), \quad (25)$$

where $\tilde{c} = c/n$ is the light velocity in the film and κ is the transparency of the film-air interface averaged over photon modes in the escape cone. This averaged film-air transparency equals to the air-film transparency averaged over the all photon modes in the air. In PV devices with back-surface mirrors, the photon emission is only realized through the film-air interface. In such devices the photon escape time is given by

$$\tau_{es} = \frac{N(T,d)}{\dot{N}_{f-a}(T)} = \frac{4d}{\tilde{c}\kappa(\sin\theta_{es})^2} = 4n^2\frac{d}{\kappa\tilde{c}}. \quad (26)$$

Thus, the photon escape via the film-air interface is suppressed by the factor $4n^2$ due to internal reflection. As it was highlighted by Yablonovitch [17, 25], the photon escape from the film-air interface is strongly limited, because the the photon flux propagating in the film is n^2 times bigger than the photon flux that can propagate in the air (the photon DOS is proportional to n^3 and the propagation rate is proportional to n^{-1}). Therefore, in solar cells with back-surface mirror the film photons are strongly trapped by mirror and the film-air interface. This trapping is consistent with high transparency of the film-air interface for the modes in the escape cone. Let us note that various photonic structures may be used to further reduce the emission angle at the film - air interface. For PV applications the limiting emission angle in the air is given by the angular radius of Sun when seen from Earth, which is 0.0046 radians (0.53 degrees) [9].

If the photon escape time, τ_{es}, is much longer than the photon absorption time, $\tau_{ab} = 1/(\alpha\tilde{c})$, where α^{-1} is the average absorption length, a film photon is reabsorbed $\tau_{es}/\tau_{ab} = 4n^2d\alpha/\kappa$ times before it leaves the film. In this case, the radiative photocarrier lifetime increases as

$$\tau_\ell^r = \frac{\tau_{es}}{\tau_{ab}}\cdot\tau_r = 4n^2\frac{d\alpha}{\kappa}\cdot\tau_r, \quad (27)$$

where τ_r is the minority carrier recombination time. The relation between the average absorption length, α, and directly measured parameters of the radiative recombination will be discussed in Section V. Assuming antireflection coating, which provides high photon absorption, we accept that $\kappa = 1$. Taking into account nonradiative recombination processes, the total photocarrier lifetime may be presented as

$$\frac{1}{\tau_\ell} = \frac{1}{\tau_\ell^r} + \frac{1}{\tau_{nr}} = \frac{1}{4n^2d\alpha\tau_r} + \frac{1}{\tau_{nr}} = \frac{1}{4n^2d\alpha k_l\tau_r}, \quad (28)$$

where τ_{nr} is the minority carrier nonradiative recombination time and k_l is the luminescence quantum yield, introduced in Eq. 5. According to Eq. 28, the luminescence quantum yield may be presented as

$$k_l = \left(1 + \frac{4n^2d\alpha\tau_r}{\tau_{nr}}\right)^{-1}. \quad (29)$$

The two-body radiative recombination rate and three-body Auger recombination rate are described by corresponding constants B_r and C_{Au},

$$\dot{R}_r = B_r\cdot n\cdot p \quad (30)$$
$$\dot{R}_{Au} = C_{Au}\cdot(n^2\cdot p + p^2\cdot n), \quad (31)$$

where n and p are electron and hole concentrations. Usually density of light-induced carriers is substantially less than density of majority carriers, i.e. the density of dopants or acceptors in the base of PV device. Then, according to Eqs. 30 and 31, the radiative recombination time and Auger recombination time are

$$\tau_r = 1/(B_rN) \quad (32)$$
$$\tau_{Au} = 1/(C_{Au}N^2), \quad (33)$$

where N is the dopant (acceptor) density. Substituting the ratio τ_r/τ_{Au} in Eq. 29 we obtain the luminescence quantum yield limited by Auger processes,

$$k_l^{Au} = \left(1 + 4n^2d\alpha\cdot\frac{C_{Au}N}{B_r}\right)^{-1}. \quad (34)$$

Thus, the three-body multiplication and recombination Auger processes are directly incorporated in the gSQ model via coefficients γ and k_l^{Au} . Eqs. 11 -16 with the parameter A (Eq. 8) reduced by k_l^{Au} (Eq. 34) describe effects of Auger processes on PV performance. For GaAs the radiative and Auger recombination constants are $B_r = 7.2 \cdot 10^{-10}$ cm^{-3} sec^{-1} [26, 27] and $C_{Au} = 10^{-30}$ cm^{-6} sec^{-1} [28]. Therefore, in GaAs PV devices with typical doping of $N = 10^{17}$ cm^{-3} the coefficient $C_{Au}N/B_r$ is $\simeq 10^{-3}$ and even in devices with strong photon recycling, $4n^2 d\alpha \sim 50$, the effect of Auger recombination is negligible. In the indirect bandgap semiconductor materials the radiative recombination is strongly suppressed and, therefore, Auger recombination is an important efficiency limiting factor. For example, for silicon the recombination constants are $B_r \simeq 10^{-14}$ cm^{-3} sec^{-1} and $C_{Au} = 10^{-30}$ cm^{-6} sec^{-1} [28]. For doping of $N = 10^{16}$ cm^{-3} the coefficient $C_{Au}N/B_r$ is $\simeq 1$. Therefore, according to Eq. 34, significant photon recycling decreases the luminescence quantum yield, $k_l^{Au} \simeq 1/(4n^2\alpha d)$. The gSQ model provides an effective tool for optimization trade-off processes, such as photon absorption (recycling and trapping) and photocarrier collection (the luminescence quantum yield).

V. Nonradiative Recombination of Interacting Photocarriers

In this section we consider PV conversion of interacting photocarriers. The Shockley-Read-Hall and other processes may provide substantial contribution to the nonradiative recombination and suppress PV efficiency. While for non-interacting photocarriers the recombination rate is proportional to the concentration of minority carriers, i.e. to $\exp(\mu/kT)$, interaction effects may result in complex dependencies of the recombination rate from the photocarrier density. In the general case, we can describe the nonradiative recombination of interacting photocarriers by the term $\dot{R}_{int} \cdot \exp(\mu/nkT)$, where $\dot{R}_{int}$ is the corresponding nonradiative recombination rate in the thermodynamic equilibrium ($\mu = 0$), and n is the ideality factor. To take into account recombination of interacting photocarriers, Eq. 6 for the electric current of non-interacting (free) photocarriers should be corrected. With an additional term, which describes recombination due to interaction of photocarriers, the electric current is given by

$$\begin{aligned} J/q &= \gamma \dot{N}_{ab} - \dot{R}_{free} \cdot \exp\frac{\mu}{kT} - \dot{R}_{int} \cdot \exp\frac{\mu}{nkT} \\ &= \dot{N}_{ab}\left(\gamma - \frac{1}{A}\cdot \ exp\frac{\mu}{kT} - \frac{1}{B}\cdot\exp\frac{\mu}{nkT}\right). \end{aligned} \quad (35)$$

where $A = \dot{N}_{ab}/\dot{R}_{free}(T) = k_l \dot{N}_{ab}/\dot{N}_{em}(T)$ (see Eqs. 5 and 8) and $B = \dot{N}_{ab}/\dot{R}_{int}(T)$.

Without nonradiative recombination induced by interaction processes the voltage at maximal efficiency is given by Eq. 10. The radiative processes may be included in Eq. 10 in the iterative way. Taking into account Eq. 35, we get

$$\begin{aligned} \frac{qV_m^i}{kT} &= \mathrm{LW}(e \cdot A^{(i-1)}) - 1, \\ \frac{1}{A^{(i-1)}} &= \frac{1}{A} + \frac{1}{B}\cdot\exp\left(\frac{1-n}{n}\cdot\frac{qV_m^{(i-1)}}{kT}\right), \end{aligned} \quad (36)$$

where in the i-iteration for V_m the parameter A is determined by the V_m, which was found at previous iteration. The corresponding efficiency is given by Eq. 11 with the corrected parameter A or, alternatively, it may be calculated by Eq. 13, which presents the efficiency via V_m.

Eq. 36 provides the general iterative solution for V_m and PV efficiency in the case of interacting electrons. If nonradiative recombination due to photocarrier interaction is slow in comparison with other radiative and nonradiative processes, the corresponding solution for V_m and PV efficiency may be found in the first iteration. In this case, the shift of the voltage at maximal power is

$$\frac{q\Delta V_m}{kT} = -\frac{A}{nB}\left(\frac{A}{\mathrm{LW}(A)}\right)^{\frac{1-n}{n}} = -\frac{\dot{R}_{nr}}{n\dot{R}_r}\left(\frac{A}{\mathrm{LW}(A)}\right)^{\frac{1-n}{n}} \quad (37)$$

and the efficiency reduction is given by

$$\begin{aligned} \Delta\eta &= -\frac{A}{B}\left(\frac{A}{\mathrm{LW}(A)}\right)^{\frac{1-n}{n}}\frac{kT}{\epsilon^*} = \frac{\dot{R}_{nr}}{\dot{R}_r}\left(\frac{A}{\mathrm{LW}(A)}\right)^{\frac{1-n}{n}}\frac{kT}{\epsilon^*} \\ &= \frac{nq\Delta V}{\epsilon^*}. \end{aligned} \quad (38)$$

As seen from Eqs. 37 and 38, if $n > 1$, effects of nonradiative recombination are strongly suppressed due to the large values of parameter A, which is the ratio of absorption rate and recombination rate. For example, for the Shockley-Read-Hall processes with the ideality factor $n = 2$, the corresponding reduction of the voltage at maximal efficiency and the reduction of conversion efficiency are

$$\frac{q}{kT}\Delta V_{SRH} = -\frac{\dot{R}_{nr}}{2\dot{R}_r}\sqrt{\frac{\mathrm{LW(A)}}{\mathrm{A}}} \quad (39)$$

$$\Delta\eta_{SRH} = -\frac{\dot{R}_{nr}}{\dot{R}_r}\sqrt{\frac{\mathrm{LW(A)}}{\mathrm{A}}}\cdot\frac{kT}{\epsilon^*}. \quad (40)$$

Let us note that in the double diode model the ratio $\dot{R}_{nr}/\dot{R}_r$ is given by the ratio of the ratio of SRH and radiative dark currents, J_{02}/J_{01}, and the parameter A is the ratio of the photocurrent to the radiative dark current, J_{ph}/J_{01}.

VI. Photocarrier Kinetics

Next, we will employ the developed formalism to kinetics of photons and electrons in a semiconductor film and calculate corresponding characteristics times and lengths. To calculate the optimal photocarrier collection rate, let us present the electric current and the recombination rate

in terms of the carrier collection time, τ_{col}, and photocarrier lifetime τ_ℓ [29],

$$J(V) = \frac{qn_0 d}{\tau_{col}(V)} \cdot \exp\frac{qV}{kT},$$
$$\dot{R}(V) = \frac{n_0 d}{\tau_\ell} \cdot \exp\frac{qV}{kT}, \quad (41)$$

where n_0 is the equilibrium concentration of minority carriers. Taking into account that $J(V)/q = \dot{N}_{ab} - \dot{R}(V)$, we may express the absorbed flux as $J\dot{N}_{ab} = \dot{R}(V_{OC})$. Thus, at the voltage that provides the maximal conversion efficiency we obtained

$$\frac{\exp(qV_m/kT)}{\tau_{col}(V_m)} = \frac{exp(qV_{OC}/kT)}{\tau_\ell} - \frac{\exp(qV_m/kT)}{\tau_\ell}. \quad (42)$$

Finally, using Eqs. 10 and 42, we find that the photocarrier collection time at optimal efficiency is given by

$$\tau_{col}(V_m) = \tau_\ell/\beta, \quad (43)$$
$$\beta = \mathrm{LW}(\gamma A) \approx \frac{qV_m}{kT}. \quad (44)$$

Fig. 3 shows the dependence of parameter β on the semiconductor bandgap for the 6000 K radiation. As seen, in the optimal conversion regime the carrier collection time is substantially shorter than the photocarrier lifetime. For example, for PV conversion of unconcentrated light with Si solar cell β equals 29 and with GaAs solar cell β equals 41. The coefficient β increases with the light concentration and reaches values of 41 for Si and 52 for GaAs PV device.

As the Shockley-Queisser model is essentially based on the detail balance between generation and recombination processes, for modeling pV devices it is critically important to use photon and electron characteristics that are consistent with the detailed balance. In equilibrium, the detailed balance between light absorption and radiative recombination processes allows one to present the photon absorption time through recombination parameters,

$$\dot{R}_r(T) = \frac{n_0 d}{\tau_r} = \frac{n_{ph} d}{\tau_{ab}}, \quad (45)$$

where n_o is the equilibrium density of minority carriers and n_{ph} is the equilibrium density of photons with energies above the semiconductor band gap (ϵ_g),

$$n_0 = \frac{(kT)^3 (m_e m_h)^{3/2}}{2\pi^3 \hbar^6 N}\, exp\left(-\frac{\epsilon_g}{kT}\right) \quad (46)$$
$$n_{ph} = \frac{n^3 \epsilon_g^2\, kT}{\pi \hbar^3 c^3}\, exp\left(-\frac{\epsilon_g}{kT}\right), \quad (47)$$

where $m_e(m_h)$ is the electron (hole) mass. Using Eqs. 45-47, we find

$$\tau_{ab} = \frac{2\pi^2}{B_r}\left(\frac{\hbar n}{\sqrt{m_e m_h} c}\right)^3 \left(\frac{\epsilon_g}{kT}\right)^2$$
$$\simeq 0.6 \cdot 10^{-30} \left(\frac{n}{(\tilde{m}_e \tilde{m}_h)^{1/2}}\right)^3 \left(\frac{\epsilon_g}{kT}\right)^2 \frac{cm^3}{B_r} \quad (48)$$

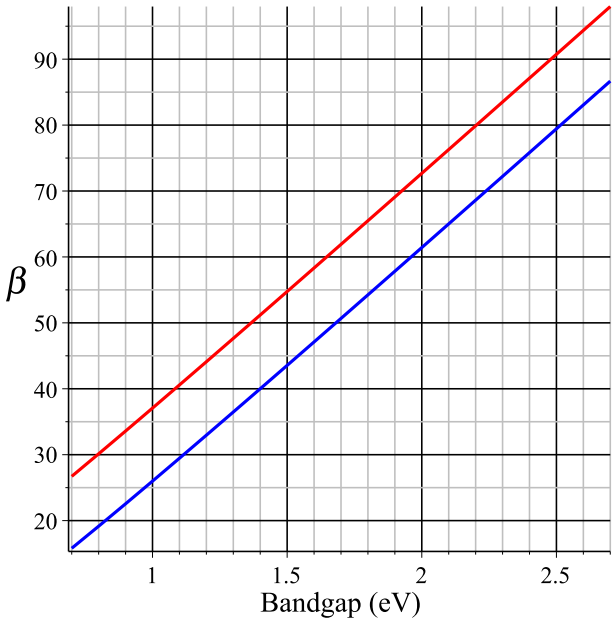

FIG. 3: The ratio of the photoelectron lifetime to the collection time at optimal PV conversion for the concentrated radiation (red) and unconcentrateted radiation (blue).

where $\tilde{m}_e(\tilde{m}_h)$ is the effective mass of electron (hole) used for density of states calculations. For example, using $B_r = 7.2 \cdot 10^{-10}$ cm^{-3} sec^{-1} [26, 27], we obtained the absorption time in GaAs is 20 fs and the corresponding absorption length, $\ell_{ab} = (c/n) \cdot \tau_{ab}$, is 1.7 μm. For silicon the radiative recombination constant is $4.73 \cdot 10^{-15}$ cm^{-3} sec^{-1} [30], which gives the absorption time of 21 ps and the absorption length of 1900 μm.

As we discussed above, Eq. 48 is direct consequence of the detailed balance between photon absorption (emission) and photocarrier generation (recombination) in the volume of a semiconductor. Another detailed balance equation is a consequence of the Kirchhoff's relation between photon emission and absorption (see Eq. 1). The photon emission from the semiconductor structure may be also presented via the photon escape time,

$$\dot{N}_{em}(\mu) = d \int \frac{1}{\tau_{es}(\omega)}\, D_\omega \exp\left(-\frac{\hbar\omega}{kT}\right) d\omega \quad (49)$$
$$= \frac{n_{ph} d}{\tau_{es}}, \quad (50)$$

where Eq. 50 defines the averaged photon escape time consistent with the detailed balance. If the photon escape is selective, this averaged time should be used in Eq. 27 together with the absorption time (Eq. 48) to calculate the photocarrier lifetime. Finally, according to Eq. 27, in the photon recycling regime the radiative photocarrier lifetime and the photocarrier lifetime with respect both radiative and nonradiative processes are given by

$$\tau_\ell^r \simeq \tau_{es} \cdot 1.6 \cdot 10^{30} \frac{(\tilde{m}_e \tilde{m}_h)^{3/2}}{n^3} \left(\frac{kT}{\epsilon_g}\right)^2 \frac{cm^3}{N}, \quad (51)$$

$$\tau_\ell \simeq \tau_{es} k_\ell \cdot 1.6 \cdot 10^{30} \ \frac{(\tilde{m}_e \tilde{m}_h)^{3/2}}{n^3} \ \left(\frac{kT}{\epsilon_g}\right)^2 \ \frac{cm^3}{N}. \quad (52)$$

As it is expected, in the photon recycling regime the radiative photocarrier lifetime is independent on exciton-photon coupling, i.e. on B_r, and proportional to the photon escape time. Therefore, the photocarrier lifetime depends on radiative and nonradiative processes solely via the luminescence quantum yield. For high quality PV materials ($k_l \sim 1$), the photocarrier lifetime in inversely proportional to the square of semiconductor bandgap and density of donors (acceptors).

VI. Diffusion Limited Photocarrier Collection

Now we will analyze model limitations related to the diffusion processes. Decrease of the open circuit voltage by diffusion processes was analyzed in a number of papers [31, 32] . For effective photocarrier collection in the regime of maximal efficiency, the film thickness, d, should be shorter than the corresponding diffusion length related to the carrier collection time, $\sqrt{D\tau_{col}}$, where D is the diffusion coefficient and τ_{col} is the optimal photocarrier collection time, which is much shorter than the photocarrier lifetime (Eqs. 43 and 44). According to Eqs. 28 and 43, the optimal photocarrier collection time may be presented as

$$\tau_{col}(V_m) = 4n^2 d\alpha k_l \cdot \frac{\tau_r}{\beta}, \quad (53)$$

where τ_r is the minority carrier radiative recombination time, introduced in Eqs. 27 and 32. Thus, the requirement of fast photocarrier diffusion to contacts may be presented in the following way,

$$d < \ell_r \sqrt{\frac{4n^2 d\alpha k_l}{\beta}}, \quad (54)$$

where ℓ_r is the minority carrier diffusion length with respect to radiative recombination, $\ell_r = \sqrt{D\tau_r}$. On the other hand, the effective light absorption requires an adequate thickness of the base. In PV devices with randomly textured front surface and back-surface mirror, the photon trapping enhanced the absorptance, which is given by $\tilde{\alpha} = 1 - \exp(-4n^2\alpha d)$. Finally, two requirements of effective absorption and fast photocarrier collection may be presented as

$$\frac{1}{4n^2\alpha} < d < \frac{4n^2\alpha\ell_r^2 k_l}{\beta}. \quad (55)$$

Thus, to provide both effective absorption and photocarrier collection, the photovoltaic material should have the characteristics that satisfy the following condition,

$$\alpha\ell_r = \frac{\ell_r}{\ell_{ab}} \gg \frac{1}{(2n)^2}\sqrt{\frac{\beta}{k_l}}. \quad (56)$$

Let us note that the one factor of $2n$ in r.h.s of Eq. 56 originates from the absorption enhancement via photon trapping and the second $2n$ factor in the denominator is due to the increase of the photocarrier lifetime via photon recycling. The factor of $\sqrt{\beta}$ in Eq. 56 takes into account that at the optimal conversion efficiency the photocarrier collection time is much shorter than the lifetime. The luminescence quantum yield, k_l in Eq. 56 takes into account decrease of photocarrier lifetime due to nonradiative processes. Let us highlight, that even in the high quality PV materials, the factor of $\sqrt{\beta/k_l}$ exceeds 10 and, therefore, without trapping and recycling the diffusion length ℓ_r should exceed the absorption length, ℓ_{ab} by more than one order in magnitude.

TABLE I: Parameters of SI and GaAs PV materials

Material	ℓ_{ab} μm	ℓ_r μm	ℓ_r/ℓ_{ab}
GaAs	1.7	7	4
Si	1900	2200	1.2

Using absorption and recombination characteristics consistent with the detailed balance (Section V), let us consider popular direct and indirect bandgap materials GaAs an Si. For high quality GaAs material, the the photoelectron diffusion coefficient, D_e is 100 cm^2/s and with typical values of emission constant $B_r = 7.2 \cdot 10^{-10}$ cm^{-3} sec^{-1} and acceptor density of $N_A = 3 \cdot 10^{17}$ / cm^{-3}, the photoelectron diffusion length, $\ell_r = \sqrt{D_e/B_r N_A}$ is 7 μm. Using the absorption length of 1.7 μm, which was calculated in the previous Section, we find the ratio $\ell_r/\ell_{ab} \approx 4$. Let us note that we calculate the ratio ℓ_r/ℓ_{ab} using a single kinetic parameter, which is the radiative recombination constant, B_r . As, the ratio ℓ_r/ℓ_{ab} is proportional to $\sqrt{B_r}$, it weakly depends on the value of B_r. The above consideration shows that without photon management even in a solar cell fabricated from the best PV material, GaAs, the photocarrier diffusion cannot provide the photocarrier collection time required for optimal PV efficiency. The same evaluations for Si with $D_e = 20$ cm^2/s and $B_r = 4.73 \cdot 10^{-15}$ cm^{-3} s^{-1} [30] are summarized in Table I.

Thus, for solar cells without photon management the absorption/diffusion trade-off (Eq. 56 without $(2n)^2$ factor in the r.h.s. denominator) can limit PV efficiency, while this trade-off is not critical for the open circuit voltage. Let us highlight again, the photocarrier collection time in the optimal power regime is substantially shorter than the photocarrier lifetime and realization of fast photocarrier collection requires faster diffusion processes and/or thinner devices. As we discussed above, effects of photon trapping and recycling reduce the r.h.s of Eq. 56 by $4n^2 \simeq 50$. Therefore, in solar cells with photon management the optimal thickness is reduced to $d \approx (3 \div 5)/(4n^2\alpha)$ and diffusion processes do not limit the optimal collection rate calculated in Section IV.

VII. GaAs Cell Operating Close to SQ Limit

In July 2018 Alta Devices announced that its most

recent single junction GaAs solar cell demonstrates PV efficiency of 28.9 %, which has been certified by NREL. During last years Alta Devices does not present details of the research, device structure, and detailed characteristics. Therefore, in this section we will analyze the Alta Device solar cell with 27.6 % efficiency presented in Ref. 33 in 2011. Under AM1.5G illumination at 1 sun intensity this GaAs cell demonstrated the following parameters: the short circuit current $J_{sc} = 29.6$ mA/cm^2, the open circuit voltage $V_{oc} = 1107$ mv, the fill factor $FF = 84.1$ %, the current at maximal power $J_m = 28.6$ mA/cm^2, and voltage at maximal power $V_m = 963$ mV. Also, the measured dark current was analyzed by the two-diode model,

$$J_d = J_{01}\left(\exp\frac{q(V - J_d R_s)}{kT}\right) + J_{02}\left(\exp\frac{q(V - J_d R_s)}{2 \cdot kT}\right), \tag{57}$$

and values of the characteristic currents were determined, $J_{01} = 6{\cdot}10^{-21}$ A/cm^2 and $J_{02} = 1{\cdot}10^{12}$ A/cm^2. Also, the dark current characteristics allow us to evaluate the series resistance in dark, $R_{s,d} = 1.8$ $\Omega{\cdot}$cm^2. The authors of Ref. 33 concluded that the effect of SRH recombination on PV efficiency is negligible and the device performance was limited by series resistance.

Let us employ the developed formalism to analyze various factors that limit PV efficiency. Above the 1.4 eV bandgap the AM1.5G illumination at 1 sun intensity provides the photon flux $\dot{N}_{flux} = 2.05 \cdot 10^{17}$ cm^{-2}s^{-1} with the average photon energy $\tilde{\epsilon} = 3.043$ eV. At temperature of 300 K, the black-body emission flux above the 1.4 eV bandgap is $\dot{N}^{bb}_{em}(T) = 0.011$ cm^{-2}s^{-1}. Thus, in SQ limit the parameter $A = \dot{N}_{ph}/\dot{N}_{em}(T)$ (Eq. 8) is $1.83 \cdot 10^{19}$. According to Eq. 10, the voltage at maximal power may be calculated as

$$qV_m = kT \cdot (\mathrm{LW}(A \cdot e) - 1), \tag{58}$$

which gives 1044 meV in SQ limit. The PV efficiency may be calculated via the parameter A by Eq. 11 or it may be calculated via V_m as

$$\eta = \tilde{\alpha}\frac{(qV_m)^2}{(qV_m + kT) \cdot \tilde{\epsilon}}, \tag{59}$$

which follows from Eq. 13. In the SQ limit the absorptance $\tilde{\alpha}$ is 1 and Eq. 59 gives the PV efficiency of 33.5 %.

The device absorptance may be evaluated as the ratio of the absorbed flux, $\dot{N}_{ab}$, corresponding to the short circuit current, $J_{sc}/q = 1.85 \cdot 10^{17}$ cm^2, to the incoming flux $\dot{N}_{flux} = 2.05 \cdot 10^{17}$ cm^{-2}. The obtained absorptance of 0.90 reduces the efficiency to 30.1 %. Assuming the Kirchhoff's relation between averaged absorptivity and emissivity, we do not expect changes in V_{oc} and V_m.

Next, let us evaluate the luminescence quantum yield. The J^r_{01} component of the dark current corresponding to the radiative recombination is $\tilde{\alpha}\dot{N}_{em}/q = 1.62 \cdot 10^{-21}$ cm^{-2}s^{-1}. Thus, the external luminescence quantum yield is $J^r_{01}/J_{01} = 0.27$. According to Eq. 8, the parameter A is reduced to $4.93 \cdot 10^{18}$. Eqs. 58 and 59 (or Eq. 11) give $V_m = 1011$ meV and efficiency of 29.2 %. As we discussed in Section IV, effect of Auger recombination processes on PV characteristics of GaAs devices is negligible. The calculated luminescence quantum yield may be associated with surface recombination and absorption of the metallic mirror.

TABLE II: Loss mechanisms and their impact on V_m and PV efficiency of GaAs solar cell

	SQ limit	Absorption	Nonradiative Processes	SRH Processes	Experiment [33]
A	$1.83 \cdot 10^{19}$	$1.83 \cdot 10^{19}$	$4.93 \cdot 10^{18}$	$2.23 \cdot 10^{18}$	
V_m	1044 meV	1044 meV	1011 meV	999 meV	963 meV
η	33.5 %	30.1 %	29.2 %	28.8 %	27.6 %

Effect of SRH recombination may be calculated in the iterative way by Eq. 36. In terms of the dark current components the i-iteration for V_m may be presented as

$$A^{(i)} = \frac{J_{sc}}{J_{01} + J_{02}\exp\left(-\frac{qV_m^{(i-1)}}{2kT}\right)}, \tag{60}$$

$$qV_m^{(i)} = kT \cdot (\mathrm{LW}(e \cdot A^{(i)}) - 1),. \tag{61}$$

The iteration process starts with the $V_m^{(0)}$, which was calculated before in zero order in SRH recombination. After several iterations we find $A = 2.23 \cdot 10^{18}$ and $V_m = 999$ meV. The PV efficiency is reduced by SRH recombination to 28.8 %. SRH processes also decrease the external quantum yield, k_l, from 0.27 to 0.19.

Finally, the reduction of V_m from 999 meV to experimental value of 963 meV may be associated with the series resistance. The corresponding value of the series resistance under illumination is evaluated as 1.3 $\Omega{\cdot}$ cm^2. The reduction in efficiency from 28.8 % to 27.6 % gives the value of series resistance of 1.4 $\Omega{\cdot}$cm^2, which is close to that evaluated from the V_m reduction. The obtained series resistance under illumination is slightly smaller than that in dark, 1.8 $\Omega{\cdot}$cm^2.

Loss mechanisms and their impact on the voltage at maximal power and PV efficiency are summarized in Table II. As seen, the measured PV efficiency is by 5.9 % below the SQ limit. The series resistance reduces efficiency by 1.1 %, the SRH processes by 0.4 %, and other nonradiative recombination processes by 0.9 %. The significant reduction of efficiency is related with limited absorption due to contact shadowing and reflectivity. The developed formalism allows experimentalists to make such analysis with a scientific calculator or popular mathematical packages.

Also, well-developed mathematical analysis of Lambert W functions allows one to simplify calculations of various PV characteristics. In particular, for $\mathrm{LW}(z) \gg 1$, the

derivative of LW(z) has a very simple form,

$$\frac{d\mathrm{LW}(z)}{dz} = \frac{\mathrm{LW}(z)}{z\cdot(1+\mathrm{LW}(z))} \approx \frac{1}{z}. \qquad (62)$$

This equation may be used for calculation of dependencies of V_m and PV efficiency on the parameters of photonic flux, temperature, and material parameters. For example, the dependence of the efficiency (Eq. 19) on the external quantum yield is given by

$$\frac{d\eta}{dk_l} = \frac{kT}{\epsilon^*}\frac{1}{k_l} = \frac{\tilde{\alpha}\cdot kT}{\tilde{\epsilon}}\frac{1}{k_l}, \qquad (63)$$

which clarifies efficiency reduction due to nonradiative recombination and SRH recombination presented in Table II.

Summary

In summary, in this work we study the generalized Shockley-Queisser model, which takes into account spectral absorption/emission characteristics, nonradiative recombination processes, and photon management. For non-interacting electrons and for electrons interacting via Auger processes (photocarrier multiplication, Eq. 3, and recombination, Eq. 34) we obtained exact analytical solution for photovoltaic efficiency (Eq. 11), output power (Eq. 12), and all other PV characteristics. The obtained solution provides mathematical base of PV conversion and endoreversible thermodynamics controlled by the chemical potential. Eq. 13 present the useful energy of an absorbed photon in terms of the photo-induced chemical potential. It generalizes the result obtained by Henry [1] for the ideal SQ model, which ignores the nonradiative recombination processes and absorption losses. Eqs. 13, 15, and 16 directly show the useful energy, emission losses, and total thermal losses (electron-phonon relaxation and nonradiative recombination) per absorbed photon. In the general case of interacting electrons, the solution of gSQ model is presented in perturbative way (Eq. 37 and 38). In particular, effects of the Shockley-Read-Hall processes on PV characteristics are described by Eqs. 39 and 40. Taking into account that for typical PV semiconductors the dimensionless parameter A (the ratio of the absorption rate to the recombination rate, Eq. 8) is huge, one can further simplify the expression for conversion efficiency (Eq. 19) and employ asymptotic series with logarithmic functions (Eq. 17). In this way PV efficiencies may be calculated with relatively simple scientific calculators. The developed formalism was applied to analyze the kinetics of photocarriers. Eq. 43 presents the universal relation between the optimal photocarrier collection time and the photocarrier lifetime with respect to all radiative and nonradiative processes. We also use the detailed balance between radiative recombination and absorption to introduce and analyze the averaged photon and photocarrier lifetimes (Eqs. 48, 51 and 52). Let us highlight that due to the short photocarrier collection time with respect to the photocarrier lifetime, the photocarrier kinetic and transport processes in the optimal power regime may differ from the processes in the open circuit regime. In particular, due to fast photocarrier collection the photon re-absorption in the optimal power regime and its effect on photocarrier diffusion are always negligible. Finally, we show that in traditional devices without photon management, it is not possible to realize simultaneously both high absorption and fast photocarrier collection, which is required by the optimal collection rate (Eqs. 43 and 44). In PV devices with enhanced photon trapping and recycling, the thickness of the base may be reduced below the characteristic value (Eq. 55), at which the diffusion processes do not limit the optimal photocarrier collection. The presented gSQ model and its solution provide effective, convenient, and flexible tool for optimization of modern PV devices with effective photon trapping [9, 34–36].

The authors wish to acknowledge Dr. Christopher Michael Waits and Dr. John Little for useful discussions. The work was supported by Army Research Laboratory.

[1] C. H. Henry, Limiting efficiencies of ideal single and multiple energy gap terrestrial solar cells, J. Appl. Phys. **51**, 4494 (1980).
[2] W. Shockley and H. J. Queisser, Detailed balance limit of efficiency of p-n junction solar cells, J. Appl. Phys. **32**, 510 (1961).
[3] W. Marx, The Shockley-Queisser paper A notable example of a scientific sleeping beauty, Ann. Phys. (Berlin) **526**, A41 (2014).
[4] C. Addison, Oral history of Hans Queisser, Computer History Museum, CHM ref. number X3453.2006 (2006). (http://archive.computerhistory.org/resources/access/text/2012/07/10265805-05-01-acc.pdf).
[5] T. Markvart and G.H. Bauer, What is the useful energy of a photon?, Appl. Phys. Lett. **101**, 193901 (2012).
[6] A. De Vos, P. T. Landsberg, P. Baruch, and J. E. Parrott, Entropy fluxes, endoreversibility, and solar energy conversion, J. Appl. Phys. **74**, 3631 (1993).
[7] A. De Vos, *Thermodynamics of Solar Energy Conversion*, Wiley-VCH, Weinheim, 2008.
[8] T. Markvart and P.T. Landsberg, Thermodynamics and reciprocity of solar energy conversion, Physica E **14**, 71 (2002).
[9] A. Polman and H. A. Atwater, Thermodynamics and reciprocity of solar energy conversion, Nature Mater. **11**, 174 (2012).
[10] U. Rau and T. Kirchartz, On the thermodynamics of light trapping in solar cells, Nature Mater. **13**, 103 (2014).
[11] A. Polman and H. A. Atwater, On the thermodynamics of light trapping in solar cells: Atwater and Polman reply, Nature Mater. **13**, 104 (2014).
[12] A. Lenert, D.M. Bierman, Y. Nam, W.R. Chan, I.

Celanovi, M. Soljai, and E.N. Wang, A nanophotonic solar thermophotovoltaic device, Nature Nanotechnology **9**, 126 (2014).

[13] S. Ruhle, Tabulated values of the ShockleyQueisser limit for single junction solar cells, Solar Energy **130**, 139 (2016).

[14] R. T. Ross, Some Thermodynamics of photochemical systems, J. of Chem. Phys. **46**, 4590 (1967).

[15] U. Rau, Reciprocity relation between photovoltaic quantum efficiency and electroluminescent emission of solar cells, Phys. Rev. B **76**, 085303 (2007).

[16] U. Aeberhard and U. Rau, Microscopic perspective on photovoltaic reciprocity in ultrathin solar cells, Phys. Rev. Lett. **118**, 247702 (2017).

[17] E. Yablonovitch, Inhibited pontaneous emission in solid-state physics and electronics, Phys. Rev. Lett. **58**, 2059 (1987).

[18] U. Rau, U. W. Paetzold, and T. Kirchartz, Thermodynamics of light management in photovoltaic devices, Phys. Rev. B **90**, 035211 (2014).

[19] A. Shabaev, A.L. Efros, and A.J. Nozik, Multiexciton generation by a single photon in nanocrystals, Nano Letters, **6**, 2856 (2006).

[20] R. M. Corless, G. H. Gonnet, D. E. G. Hare et al., On the LambertW function, Advances in Computational Mathematics **5**, 329 (1996).

[21] I. Chatzigeorgiou, Bounds on the Lambert function and their application to the outage analysis of user cooperation, IEEE Communications Letters. **17**, 1505 (2013).

[22] M. A. Green, Solar cell fill factors-general graph and empirical expressions, Solid-State Electronics **24**, 788 (1981).

[23] M. A. Green, *Solar Cells: Operating Principles, Technology, and System Applications* , Englewood Cliffs, NJ, Prentice-Hall, Inc., 1982. 288 p.

[24] R. M. Corless, G. H. Gonnet, D. E. G. Hare, and D. J. Jeffrey, Lambert's W function in Maple, The Maple Technical Newsletter. MapleTech. **9**, 12 (1993).

[25] O. D. Miller, E. Yablonovitch, and S. R. Kurtz, Strong internal and external luminescence as solar cells approach the ShockleyQueisser limit, IEEE Photovoltaics **2**, 303 (2012).

[26] Y. P. Varshni, Band-to-band radiative recombination in groups IV, VI, and III-V semiconductors, Phys. Status Solidi (b) **19**, 459 (1967).

[27] X. Wang, M. R. Khan, J. L. Gray, M. A. Alam, and M. S. Lundstrom, Design of GaAs solar cells operating close to the ShockleyQueisser limit, IEEE Photovoltaics **3**, 737 (2013).

[28] *Handbook Series on Semiconductor Parameters Volume 1: Si, Ge, C (Diamond), GaAs, GaP, GaSb, InAs, InP, InSb* edt. M. Levinshtein, S. Rumyantsev, and M. Shur, World Scientific, 1996.

[29] A. Varghese, M. Yakimov, V. Tokranov, V. Mitin, K. Sablon, A. Sergeev, and S. Oktyabrsky, Complete voltage recovery in quantum dot solar cells due to suppression of electron capture, Nanoscale **8**, 7248 (2016).

[30] T. Trupke, M. A. Green, P Wrfel et al., Temperature dependence of the radiative recombination coefficient of intrinsic crystalline silicon, J. Appl. Phys. **94**, 4930 (2003).

[31] S.R. Forrest, The limits to organic photovoltaic cell efficiency, MRS Bulletin **30**, 28 (2005).

[32] M. Gioannini, A.P. Cedola, N. Di Santo, F. Bertazzi, and F. Cappelluti, Simulation of quantum dot solar cells including carrier intersubband dynamics and transport, IEEE Journal of Photovoltaics **3**, 1271 (2013).

[33] B. M. Kayes, H. Nie, R. Twist, S. G. Spruytte, F Reinhardt, I. C. Kizilyalli, and G. S. Higashi, 27.6 % conversion efficiency: a new record for single-junction cells under 1 sun illumination, Photovoltaic Specialists Conference (PVSC), 2011 37th IEEE, 000004 (2011).

[34] P. Bermel, C. Luo, L. Zeng et al., Improving thin-film crystalline silicon solar cell efficiencies with photonic crystals, Optics Express **15**, 16986 (2007).

[35] J. N. Munday and H. A. Atwater, Large integrated absorption enhancement in plasmonic solar cells by combining metallic gratings and antireflection coatings, Nano Letters **11**, 2195 (2010).

[36] J. Grandidier, D. M. Callahan, J. N. Munday, H. A. Atwater, Light absorption enhancement in thin-film solar cells using whispering gallery modes in dielectric nanospheres, Advanced Materials **23**, 1272 (2011).